RASĀYAN *J. Chem.*
150-157| Special Issue | 2022
ISSN: 0974-1496 | e-ISSN: 0976-0083 | CODEN: RJCABP
http://www.rasayanjournal.com
http://www.rasayanjournal.co.in

# MOLECULAR STRUCTURE AND COMPUTATIONAL STUDIES OF 1,2–BIS(4-PYRIDYL)ETHANE: 2–NITROBENZENE–1,3,5–TRIOL: AN ORGANIC ADDUCT

**C. Kohila[1], G. Dinesh Kumar[1,✉], G. Kavitha[1] and S. Jyothi[2]**
[1]Department of Chemistry, Gobi Arts & Science College, Gobichettipalayam-638 453, (Tamilnadu) India
[2]Department of Chemistry, Kumaraguru College of Technology, Coimbatore-641 006, (Tamilnadu) India
✉Corresponding Author: dineshchem@gascgobi.ac.in

**ABSTRACT**
The molecular adduct crystals of 1,2–bis(4-pyridyl)ethane:2–nitrobenzene–1,3,5–triol were synthesized by slow evaporation solution growth method at ambient temperature. The structure of molecular adduct crystal was validated by a Single crystal X-ray diffraction study and it manifests that the adduct crystal belongs to the o triclinic system with space group P1. Computational studies were carried out to understand the nature of the crystals. The various hydrogen bonding interactions were confirmed by Hirshfeld surface analysis.
**Keywords:** Adduct, Slow Evaporation, Single Crystal, Computational, Hirshfeld Surface Analysis.
RASĀYAN *J. Chem.*, Special Issue, 2022
The Manuscript focusing **SDG-9**: Industry, Innovation and Infrastructure

## INTRODUCTION

The knowledge of crystal growth processes is nowadays predominantly applied in the scientific and medical fields.[1] The acid–base crystals of organic and inorganic compounds play a crucial role in crystal growth because of their technological applications.[2] Distinctly, organic crystals provide many benefits owing to their delocalized π–electron system, high optical susceptibility, ultra-fast response, high non–linearity frequency conversion, and high optical thresholds for laser power.[3,4] Especially the inter and intra-molecular hydrogen bonding interactions are responsible for the construction of supramolecular organic crystals.[5,6] Aromatic carboxylic acids, phenolic groups, and heterocyclic rings with nitrogen atoms are employed for generating supramolecular assembly via hydrogen bonding interactions by transferring protons and co-crystals.[7-10] Based on this, we synthesized an organic adduct of 1,2-bis(4-pyridyl) ethane:2–nitrobenzene–1,3,5–triol (BPE: NBT) crystals.

## EXPERIMENTAL

Analar grade reagents of 1,2–bis(4–pyridyl)ethane (BPE) and 2–nitrobenzene–1,3,5–triol (NBT) were used for the synthesis of the adduct crystal. The equimolar composition of the two reactants was dissolved individually in methanol and blended collectively. The resultant solution was mixed well for 1 hour using a magnetic stirrer. After stirring, Whatman filter paper was used to filter off the impurities from the solution. The filtered clear solution was retained in a beaker without any disturbance in a room temperature for the crystal growth. After 15 days, clear, well–defined crystals were collected. The harvested crystals were subjected to repeat recrystallization to enhance the quality of the crystal (Scheme-1).

## RESULTS AND DISCUSSION

### Single Crystal X-ray Diffraction Analysis

The co-crystals of BPE: NBT crystallizes in a triclinic system with an enantiomeric space group, P1. Figure-1 shows the ORTEP view of the adduct and the crystallographic information is given in Table-1. The asymmetric unit has a molecule of 1,2-bis(4-pyridyl)ethane and 2-nitrobenzene-1,3,5-triol which forms a 2D network with a C-H…π interaction and a C-H…O interaction. The prominent former interaction arises from the phenylic hydrogen with the neighboring pyridyl ring while the latter arises from the ethylene hydrogen with one of the hydroxyl hydrogens of the triol moiety. The


http://doi.org/10.31788/RJC.2022.1558218

BPE molecule inclined 55.95º towards the NBT molecule to form such interactions. The presence of the nitro group promotes an additional interaction in the form of N-O…π interactions as observed in the literature.[11] The pyridyl ring connected through ethane for BPE and a nitro group containing triol ring for NBT promotes a variety of non-covalent interactions in the BPE: NBT molecule.

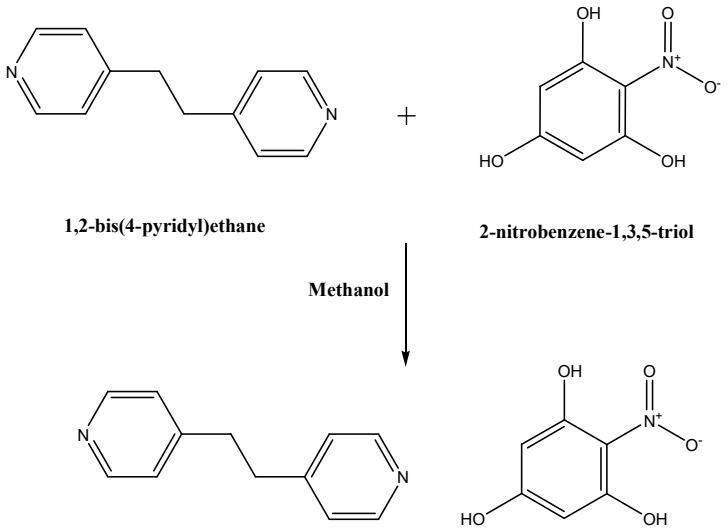


Scheme-1

The BPE: NBT molecule is stabilized with a variety of intermolecular interactions *viz*., π…π, C-H…π, N-O…π (nitro...π), O-H…O, O-H…N, C-H…O interactions extend the molecule to a three-dimensional network. The existence of the nitro group in the triol molecule is an interesting phenomenon for the BPE: NBT molecule as it gives rise to numerous interactions. The major non-covalent interactions for BPE: NBT is π…π interactions which arise majorly among the pyridyl rings. This is clearly visible on extending the molecule on the 'c' axis. The centroid…centroid distance for the two pyridyl rings is 3.6026 Å (Symmetry Operation: 1-x, -y, 1-z). There arises other notable π…π interactions among the triol moieties. However, the distances are longer than the previous interactions (4.1584(14) Å). This is because C3-H3A…π interactions arise from C3-H3A of triol moiety with the neighboring pyridyl moiety (r = 2.766 Å; symmetry operation: x, y, z). It is no surprise that the presence of the nitro group produces notable non-covalent N-O…π interactions.[12,13] However, there is a unique phenomenon observed for BPE: NBT molecule. The nitro group of NBT moiety forms N2-O4…π with the neighboring NBT moiety (r= 3.5339 Å; ∠84. 94º; Symmetry operation: 2-x, 1-y, -z). In general, the nitro…π interactions arise for the phenyl ring with the nitro group attached which led to a distortion of the nitro group in relation to the phenyl ring attached. In the case of BPE: NBT, the nitro group is not distorted and differs from other molecules in the literature.[14-17] This is because of the intramolecular hydrogen bonding forms from the hydroxyl group in 1$^{st}$ and 3$^{rd}$ positions, O1-H1 and O2-H2 of NBT moiety with the nitro group, viz., O1-H1…O5, O1-H1…N1, O2-H2…O4 and O2-H2…N2. The other hydroxyl group present in the 5$^{th}$ position forms O3-H3…N1 intermolecular hydrogen bonding with the neighboring pyridyl moieties. The geometric parameters of non-covalent and hydrogen bonding interactions are specified in Table-2. Thus, the several intra and intermolecular hydrogen bonding observed led the molecule to form a 3D network of interactions that stabilize the molecule.

Table-1: Crystallographic Data for BPE: NBT

| | |
|---|---|
| Chemical formula | $C_{12}H_{11}N_2O_5$ |
| $M_r$ | 263.23 |
| Crystal system, space group | Triclinic, *P*1 |
| Temperature (K) | 298 |

| | |
|---|---|
| *a*, *b*, *c* (Å) | 7.1983 (9), 7.8513 (13), 10.2235 (14) |
| α, β, γ (°) | 90.699 (10), 91.907 (13), 94.870 (14) |
| *V* (Å$^3$) | 575.32 (14) |
| *Z* | 2 |
| Radiation type | Mo *K*α |
| μ (mm$^{-1}$) | 0.12 |
| Crystal size (mm) | 0.20 × 0.20 × 0.20 |
| Diffractometer | Rigaku Mercury 375R (2x2 bin mode) |
| Absorption correction | Multi-scan |
| $T_{min}$, $T_{max}$ | 0.575, 1.000 |
| No. of measured, independent and observed [$I > 2\sigma(I)$] reflections | 5408, 2305, 1538 |
| $R_{int}$ | 0.070 |
| $(\sin \theta/\lambda)_{max}$ (Å$^{-1}$) | 0.649 |
| $R[F^2 > 2\sigma(F^2)]$, $wR(F^2)$, $S$ | 0.055, 0.163, 0.89 |
| No. of reflections | 2305 |
| No. of parameters | 172 |
| H-atom treatment | H-atom parameters constrained |
| $\Delta\rho_{max}$, $\Delta\rho_{min}$ (e Å$^{-3}$) | 0.28 −0.26 |
| CCDC No. | 2067277 |

Table-2: Non-Covalent and Hydrogen Bond Interactions in BPE: NBT

| Donor...Acceptor | D - H (Å) | H...A (Å) | D...A (Å) | D-(H)...A (º) | Symmetry |
|---|---|---|---|---|---|
| O1-H1...O5 | 0.82 | 1.83 | 2.541(2) | 145 | - |
| O1-H1...N2 | 0.82 | 2.42 | 2.865(2) | 115 | - |
| O2-H2...O4 | 0.82 | 1.86 | 2.563(2) | 143 | - |
| O2-H2...N2 | 0.82 | 2.45 | 2.882(3) | 114 | - |
| O3-H3...N1 | 0.82 | 1.81 | 2.599(3) | 160 | 1+x, y, z |
| C5-H5...O1 | 0.93 | 2.51 | 3.268(3) | 139 | 1+x, y, z |
| C11-H11...O5 | 0.93 | 2.41 | 3.342(3) | 177 | 1-x,1-y, -z |
| C3-H3A…π | 0.93 | 2.77 | 3.517(3) | 139 | X, Y, Z |
| Cg1…Cg1 | - | - | 3.6026(14) | - | 1-X, -Y,1-Z |
| Cg1…Cg2 | - | - | 4.7623(15) | - | X, Y, Z |
| Cg2…Cg1 | - | - | 5.0753(15) | - | 2-X,1-Y,1-Z |
| Cg2…Cg2 | - | - | 4.1584(14) | - | 2-X,1-Y, -Z |
| N2 -O4…π | - | - | 3.650(2) | - | 2-X,1-Y, -Z |

**Hirshfeld Surface Analysis**

The BPE: NBT molecule is subjected to Hirshfeld surface analysis with a view to understanding and assessing the non-covalent intra and intermolecular interactions.[18] The $d_i$ and $d_e$ plots mapped on Hirshfeld surfaces (Fig.-2) denote the hydrogen donor and acceptor sites present in BPE: NBT molecule through their faint red spots over the regions. It is noted that the active hydrogen sites have clearly visible on the $d_{norm}$ surface with dark red spots. The surface with normalized distance picture outs the active sites for hydrogen bonding interactions. The dark red spots were observed over the pyridyl heterocyclic nitrogen as well the hydroxyl hydrogens of the NBT moieties. The 2D fingerprints (Fig.-3) quantify the proportions of various intermolecular interactions involved in the BPE: NBT molecule. It is noted that H…N/N…H and

O…H/H…O contacts found to contribute 9.3% and 32.0 % respectively dominate the molecular contacts. This is due to the intramolecular O-H…O and intermolecular O-H…N, C-H…O interactions as indicated in the single crystal XRD analysis.

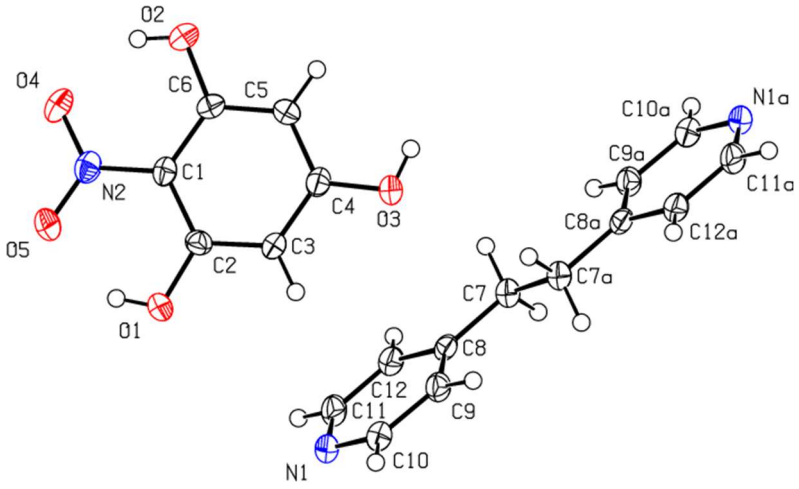


Fig.-1: ORTEP View of BPE: NBT

In total, these hydrogen bonding interactions contribute around 41.3% of the contact to the total Hirshfeld surfaces. This hydrogen bonding interactions form $R_3^3(15)$, $R_4^4$ (18), $R_4^4$ (15) ring graph pattern and intramolecular S(6) pattern of hydrogen bonding interactions links both BPE and NBT moieties. These Hydrogen bonding interactions are observed as a couple of spikes in the fingerprint plot for BPE: NBT. The H…H contacts contribute 28.3% to the total surfaces due to the rich phenyl hydrogens. The Hirschfeld Surfaces and the respective fingerprint plots for BPE: NBT is shown in Fig.-2 and 3. The C-H…π and π…π stacking interactions present in the compound lead to an increase in the C…H/H…C and C…C associated with 17.5% and 4.9 % respectively. The distance between the BPE: NBT molecular centroids (mean atomic position) calculated is R= 6.36 Å in which the total energy for the sum of four components is -14.7 kJ/mol. The energies for each component, $E_{ele}$, $E_{pol}$, $E_{dis}$, and $E_{rep}$[19,20] are found to be -2.5, -1.2, -24.4, and 16.3 respectively for the molecule considered for calculation using Crystal Explorer. The stacking interactions have been observed as a wing in the fingerprint plot. The curvedness surface with a large flat region and the design of alternate red and blue triangles in shape index with 3-fold symmetry indicates the nature of stacking in BPE: NBT. As observed for other nitro derivates in the literature, BPE: NBT has strong O…C/C…O contacts which contribute 3.6 % arises due to the presence of N2-O4…π interactions. Other contacts observed for BPE: NBT is N…C/C…N and O…O which contribute 2.0% and 1.7% respectively.

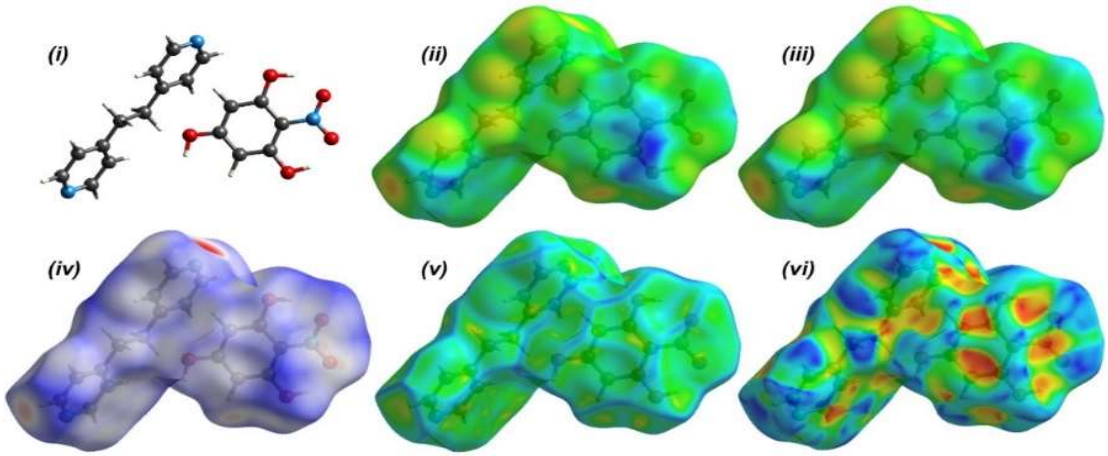


Fig.-2: (i) Molecular Structure and Hirshfeld surfaces mapped on (ii) $d_i$ (iii) $d_e$ (iv) $d_{norm}$ (v) shape index and (vi) curvedness

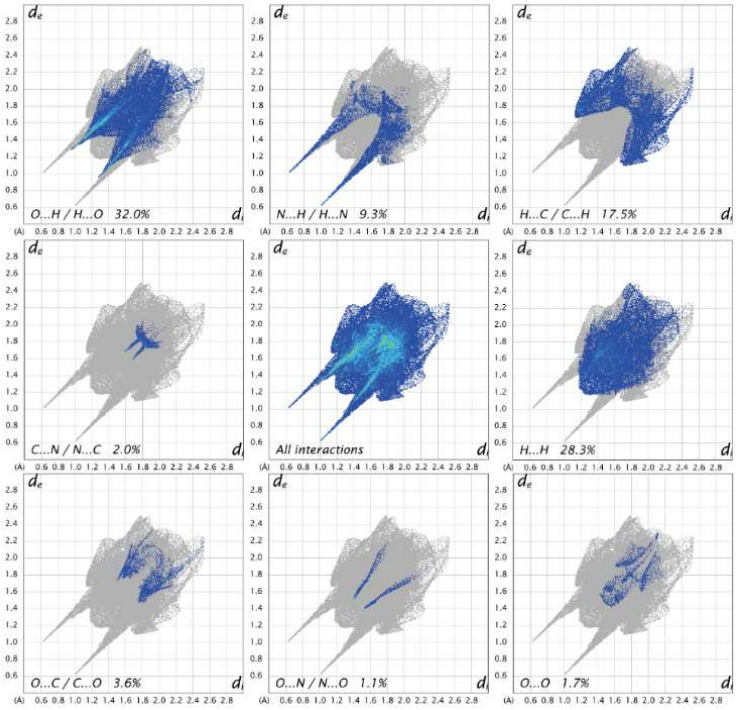


Fig.-3: Fingerprint Scheme of BPE: NBT

**Optimized Geometry**

The optimized geometry of the BPE: NBT molecule is given in the Fig.-4. It is noted that the ethane group that connects two pyridyl rings is distorted while optimizing the molecule at B3LYP/6-311G (d, p) level. However, it is noticed through X-ray diffraction for the BPE: NBT molecule, the ethane group lies in the plane of pyridyl rings. For the optimized molecule, the dihedral angle for the ethane group and the connected phenyl rings are found to be 89.02º which is completely perpendicular with respect to the ethane group. This type of distortion has also been observed by Kurt and Yurdakul[21] while optimizing 1,2-bis(4-pyridyl)ethane through DFT calculations. This causes the differences in the torsion angles for the atoms connected with the ethane group. This is due to the simulation of molecules in the gas phase. All other geometrical specifications are seen to match the experimental values. The interesting O-H…O intramolecular interactions are evidenced from the optimized molecule as well. The nitro group has also been in the same plane of the triol moiety as observed in experimental data. Even though strong intramolecular interactions were found for the triol moiety, it has N-O…π interactions. These intramolecular interactions involving the nitro group are not prominent for 2-nitroresorcinol derivatives as the distortion of the nitro group causes multiple N-O…π interactions with the neighboring molecule.

**Molecular Electrostatic Potential**

The Molecular electrostatic potential for BPE: NBT has been simulated along with the reactants, BPE, and NBT molecules. The comparative representation of MEP along with the contour mapping for BPE: NBT has been given in Fig.-5. For the BPE molecule, a strong negative potential was observed for both the nitrogen of the pyridyl ring. Also, for the NBT molecule, strong electropositive interactions over the free hydroxyl group in the 5$^{th}$ position of triol moiety. The hydroxyl group in the 3$^{rd}$ position is found to have neutral potential (White color) on account of O-H…O intramolecular interactions. The formation of the adduct makes some changes in the electrostatic potential for BPE: NBT which ends up with a mixed potential in various positions. The strength of electronegative potential for BPE: NBT has been reduced compared to the BPE molecule. However, it is available as a hydrogen acceptor (light red spots). The free hydroxyl group in BPE: NBT is highly electropositive and can establish strong hydrogen bonding interactions with the pyridyl moiety. The other two hydroxyl groups are found to be neutral owing to the development of intramolecular hydrogen bonding interactions. The contour mapping illustrates the fact of hydrogen bonding interactions and the nature of electrostatic potential found for BPE: NBT.

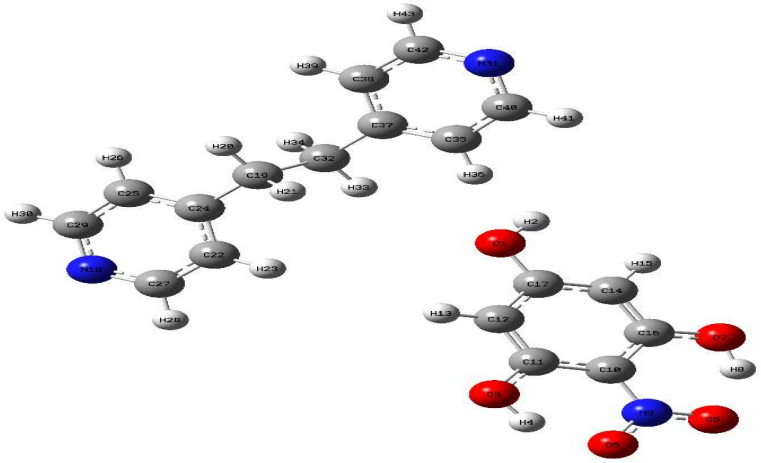

Fig.-4: Optimised Geometry of BPE: NBT

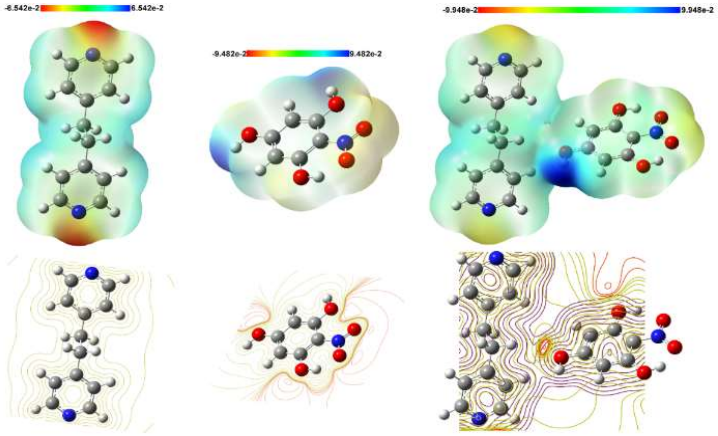

Fig.-5: Molecular Electrostatic Potential and Contour Mapping of (i) 1,2-Bis(4-pyridyl) Ethane (ii) 2-nitrobenzene-1,3,5-triol and (iii) BPE: NBT

**Theoretical UV Analysis**

The electronic absorption for BPE: NBT was evaluated theoretically by making use of DFT techniques at the B3LYP/6-311G (d, p) level of the basis set. A strong peak around 306 nm and a small hump around 409 nm are prominent in the absorption spectrum. The former band occurs with an oscillator strength of 0.2642 because of the transitions of HOMO-3 → LUMO (45%), HOMO-2 → LUMO (32%), and HOMO-1→ LUMO (20 %).

The latter has been observed on account of the charge transfer transition (HOMO → LUMO (99 %)) of the BPE: NBT molecule with an oscillator strength of 0.0258. The gap in the energy band between the HOMO and LUMO is seen to be 0.1373 a. u (3.736 eV) for BPE: NBT. Figure-6 represents the trend of BPE: NBT molecule during different transitions. The UV spectrum has been given in the inset of Fig.-6. The excitation occurs near the visible region and the lower energy gap found for BPE: NBT reveals the suitability of the molecular having optical properties.

## CONCLUSION

The co-crystals of 1,2-bis(4-pyridyl)ethane: 2-nitrobenzene-1,3,5-triol adduct has been crystallized in an enantiomeric space group. The interesting features of the molecule have been identified through Single crystal X-ray diffraction and Hirshfeld surface analysis. It is found that the molecule is stabilized by various inter and intra-molecular interactions such as C-H…π, N-O…π, π…π, C-H…O, O-H…O and O-H…N interactions. The presence of the nitro group in the NBT molecule and the aromatic framework in both moieties favor the mentioned interactions.

The Hirshfeld surfaces and corresponding 2D fingerprints point out the influence of nitro group interactions which contributes 4.0 % to the total interactions. From the optimized geometry, it is found that the π…π interactions are also prominent in the molecule. The lower band gap in theoretical UV analysis and a small hump near the visible region reveals the charge transfer interactions in BPE: NBT molecule. The charge transfer interactions are responsible for the microscopic optical properties of the molecule. Thus, the molecule can be explored for further non-linear optical applications.

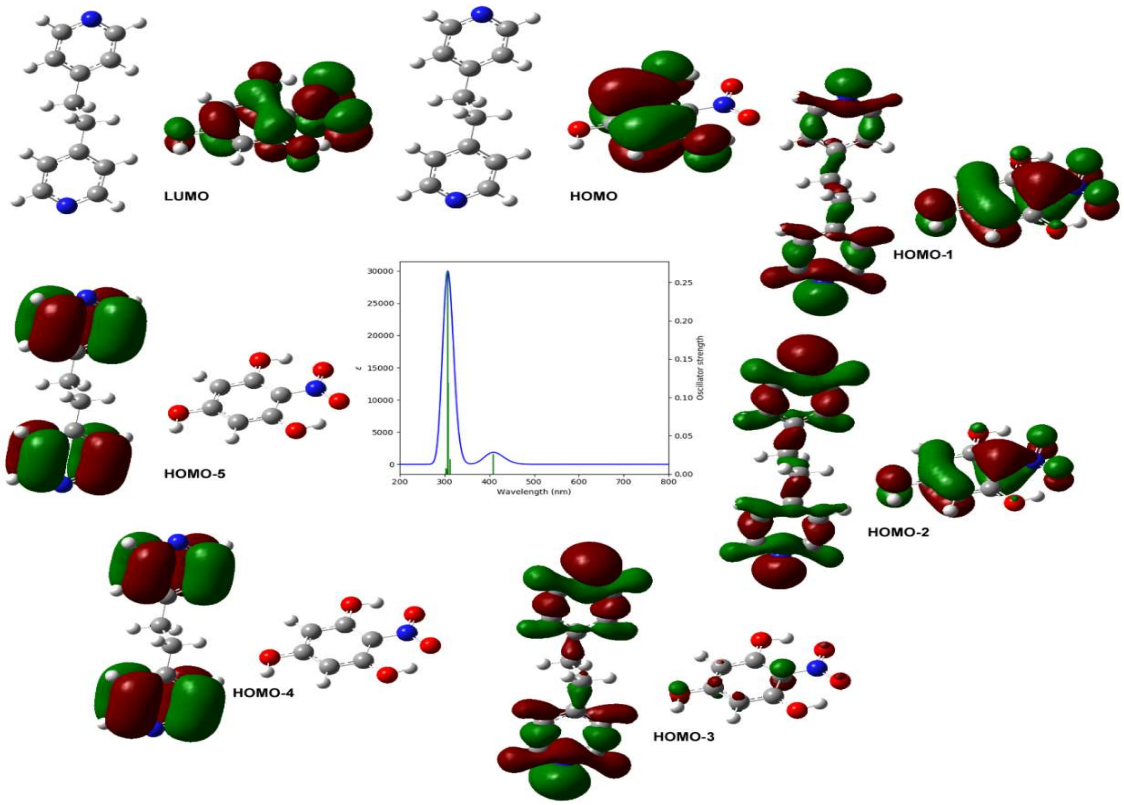


Fig.-6: Theoretical UV Spectrum of BPE: NBT at B3LYP/6-311G(d,p) Level of Theory

## ACKNOWLEDGEMENTS

We gratefully acknowledge the Common Instrumentation Centre funded by DST-FIST Scheme in Gobi Arts & Science College, Gobichettipalayam.

## CONFLICT OF INTERESTS

The authors declare that there is no conflict of interest.

## AUTHOR CONTRIBUTIONS

All the authors contributed significantly to this manuscript, participated in reviewing/editing, and approved the final draft for publication. The research profile of the authors can be verified from their ORCID ids, given below:

C. Kohila https://orcid.org/0000-0002-0715-2379
G. Dinesh Kumar https://orcid.org/0000-0002-7219-898X
G. Kavitha https://orcid.org/0000-0003-3794-4171
S. Jyothi https://orcid.org/0000-0002-4451-9723

## REFERENCES

1. D.S. Chemla and J. Zyss, Non-linear Optical Properties of Organic Molecules and Crystals, Academic Press, New York, **2** (1987), https://doi.org/10.1016/B978-0-12-170612-8.X5001-9
2. S. Madhankumar, P. Muthuraja and M. Dhandapani, *Journal of Molecular Structure,* **1203**, 127415 (2020), https://doi.org/10.1016/j.molstruc.2019.127415
3. K.S. Ramesh, M. Saravanabhavan, M. Rajkumar, D. Edison, M. Sekar, S. Muhammad and Abdullah G. Al-Sehemi, *Optical Materials*, **96**, 109341(2019), https://doi.org/10.1016/j.optmat.2019.109341
4. T. Daisyrani, M. Rajkumar and A. Chandramohan, *Materials Letters,* **222**, 118(2018), https://doi.org/10.1016/j.matlet.2018.03.195
5. Shouwen Jin, Daqi Wang, Yanfei Huang, Hao Fang, Tianyi Wang, Peixia Fu and Liangliang Ding, *Journal of Molecular Structure,* **1017**, 51(2012), https://doi.org/10.1016/j.molstruc.2012.02.048
6. R. Anitha, M. Gunasekaran, S. S. Kumar and S. Athimoolam, *Journal of Chemical Sciences,* **127**, 1435(2015), https://doi.org/10.1007/s12039-015-0914-y
7. K. Singaravelan, A. Chandramohan, S. Madhankumar, M. V. Enoch and G. vinitha, *Journal of Molecular Structure,* **1194**, 57(2019), https://doi.org/10.1016/j.molstruc.2019.05.028
8. RO.MU. Jauhar and P. Murugakoothan, *Science and Technological Research Journal*, **1**, 34(2017).
9. T. H. Duong, S. Nobusue and H. Tada, *Journal of Crystal Growth,* **537**, 125577(2020), https://doi.org/10.1016/j.jcrysgro.2020.125577
10. Lalit Rajput, Ramkinkar Santra and Kumar Biradha, *Australian Journal of Chemistry*, **63**, 578(2010), https://doi.org/10.1071/CH09415
11. E.J. Chan, S. Grabowsky, J.M. Harrowfield, M.W. Shi, B.W. Skelton, A.N. Sobolev and A. H. White, *CrystEngComm.* **16,** 4508(2014), https://doi.org/10.1039/C4CE00095A
12. P. Muthuraja, M. Sethuram, T. Shanmugavadivu and M. Dhandapani, *Journal of Molecular Structure,* **1122,** 146(2016), https://doi.org/10.1016/j.molstruc.2016.05.083
13. J.A. Kitchen, P.N. Martinho, G.G. Morgan and T. Gunnlaugsson, *Dalton Transactions,* **43,** 6468(2014), https://doi.org/10.1039/C3DT53323A
14. A. Bauza, A.V. Sharko, G.A. Senchyk, E.B. Rusanov, A. Frontera and K.V. Domasevitch, *CrystEngComm*. **19,** 1933(2017), https://doi.org/10.1039/C7CE00267J
15. P. Muthuraja, T. Joselin Beaula, T. Shanmugavadivu, V. Bena Jothy and M. Dhandapani, *Journal of Molecular Structure,* **1137,** 649(2017), https://doi.org/10.1016/j.molstruc.2017.02.067
16. S. Balachandar, M. Sethuram, P. Muthuraja, T. Shanmugavadivu and M. Dhandapani, *Journal of Photochemistry and Photobiology B: Biology*, **163,** 352(2016), https://doi.org/10.1016/j.jphotobiol.2016.08.045
17. T. Shanmugavadivu, K. Senthilkumar, M. Dhandapani, P. Muthuraja, S. Balachandar and M. Sethu Raman, *Journal of Physics and Chemistry of Solids,* **111,** 82(2017), https://doi.org/10.1016/j.jpcs.2017.07.015
18. P.R. Spackman, M.J. Turner, J.J. McKinnon, S.K. Wolff, D.J. Grimwood, D. Jayatilaka and M.A. Spackman, *Journal of Applied Crystallography,* **54,** 1006(2021), https://doi.org/10.1107/S1600576721002910
19. A. Saeed, U. Flörke, A. Fantoni, A. Khurshid, H. Pérez and M.F. Erben, *CrystEngComm,* **19,** 1495(2017), https://doi.org/10.1039/C6CE02619B
20. A. Saeed, A. Khurshid, U. Flörke, G.A. Echeverría, O.E. Piro, D.M. Gil, M. Rocha, A. Frontera, A. Mumtaz, H. El-Seedi and M.F.F. Erben, *New Journal Chemistry,* **44,** 19541(2020), https://doi.org/10.1039/D0NJ03958F
21. M. Kurt and S. Yurdakul, *Journal of Molecular Structure,* **654,** 1(2003), https://doi.org/10.1016/S0022-2860(03)00185-6

[RJC-8218/2022]